Spectrally Efficient Multicarrier Transmission With Message-Driven Subcarrier Selection

Tianlong Song, Tongtong Li, *Senior Member, IEEE*, and Jitendra K. Tugnait, *Fellow, IEEE*

***Abstract*—This paper develops two spectrally efficient orthogonal frequency division multiplexing (OFDM)-based multicarrier transmission schemes: a scheme with message-driven idle subcarriers (MC-MDIS) and another with message-driven strengthened subcarriers (MC-MDSS). The basic idea in MC-MDIS is to carry part of the information, which is named carrier bits, through an idle subcarrier selection while regularly transmitting the ordinary bits on all the other subcarriers. When the number of subcarriers is much larger than the adopted constellation size, higher spectral and power efficiency can be achieved compared with OFDM. The reason is that each idle subcarrier carries more bits than a regular symbol, with no power consumption. Moreover, the existence of idle subcarriers can also decrease possible intercarrier interference between their neighboring subcarriers. In MC-MDSS, the idle subcarriers are replaced by strengthened subcarriers, which, unlike idle subcarriers, can carry both carrier bits and ordinary bits. Therefore, MC-MDSS achieves even higher spectral efficiency than MC-MDIS. Both theoretical analysis and numerical results are provided to demonstrate the performance of the proposed schemes.**

***Index Terms*—Multicarrier transmission, OFDM, high spectral efficiency, message-driven subcarrier selection.**

I. Introduction

In conventional multicarrier transmission systems, spectral overlaps between neighboring carriers are usually avoided to eliminate intercarrier interference (ICI). When it was realized that the spectral efficiency could be significantly increased by allowing spectral overlaps between orthogonal subcarriers [1], especially after a low-cost implementation using IFFT/FFT blocks was proposed [2], orthogonal frequency division multiplexing (OFDM) has become one of the most effective ways in modern communications and is adopted by many recent standards [3], e.g., LTE [4] and WiMAX [5]. Besides the robustness to multipath fading over frequency selective channels [6], the very first advantage making OFDM prevalent is its high spectral efficiency, which is so far believed to be the highest due to the wisely introduced spectral overlap. However, there is always a question which greatly attracts the interest of many researchers: can the efficiency of a system be even higher than OFDM?

In literature, researchers have proposed to improve the efficiency of OFDM through cyclic prefix (CP) optimization [7]–[10]. In this paper, we take a different perspective and introduce two highly efficient OFDM-based multicarrier transmission schemes, which offer a positive answer to the question above. Our approaches are motivated by the idea of embedding information in channel state control [11]–[14], of which the concept of message-driven frequency hopping (MDFH) [11] gives us the most direct inspiration. In MDFH, besides carrying ordinary bits as usual, the active hopping carrier itself is specified by additional information bits and recovered by a filter bank at the receiver. Refined versions of MDFH were proposed and analyzed in [15]–[18]. For MDFH, transmission through hopping frequency control adds another dimension to the signal space, and the resulted coding gain can increase the spectral efficiency of conventional frequency hopping (FH) systems [19] by multiple times. This motivates us to improve the spectral efficiency of OFDM by allowing part of the information bits being transmitted through carrier frequency selection.

First, we propose a multicarrier transmission scheme with message-driven idle subcarriers (MC-MDIS). The basic idea is to use part of the information bits, named carrier bits, to specify idle subcarriers while transmitting ordinary bits regularly on all the other subcarriers. In this way, if the number of subcarriers is much larger than the adopted constellation size (e.g., in most OFDM systems), we can transmit more information bits at an even lower power consumption. This is because the number of carrier bits transmitted through each idle subcarrier is more than that of the ordinary bits carried by each regular symbol, and all the carrier bits are transmitted with no power consumption through idle subcarrier selection. When applied to the OFDM framework, i.e., using orthogonal subcarriers and IFFT/FFT blocks, MC-MDIS can achieve an even higher spectral efficiency than OFDM, while keeping a higher power efficiency. The existence of idle subcarriers can also decrease possible intercarrier interference (ICI) between their neighboring subcarriers. We would like to point out that, under very low SNRs, an error in idle subcarrier detection may lead to possible bit vector disorder, since the location of the idle subcarrier has a great impact on bit vector reorganization. However, this issue is properly resolved by a bit vector rearrangement (BVR) algorithm, which can be implemented with no sacrifice on spectral efficiency.

An alternative scheme, with message-driven strengthened subcarriers (MC-MDSS), is proposed simply by replacing the idle subcarriers in MC-MDIS with strengthened ones. In

Manuscript received November 19, 2013; revised March 20, 2014; accepted May 6, 2014. Date of publication May 16, 2014; date of current version July 18, 2014. This work was supported in part by the NSF under Grants CNS-0746811, CNS-1117831, CNS-1217206, and ECCS-1232109. This paper was presented in part at the 2013 IEEE GLOBECOM conference, Atlanta, GA, USA, December 2013. The associate editor coordinating the review of this paper and approving it for publication was Y. J. (Angela) Zhang.

T. Song and T. Li are with the Department of Electrical and Computer Engineering, College of Engineering, Michigan State University, East Lansing, MI 48824 USA (e-mail: songtia6@msu.edu; tongli@egr.msu.edu).

J. K. Tugnait is with the Department of Electrical and Computer Engineering, Samuel Ginn College of Engineering, Auburn University, Auburn, AL 36849 USA (e-mail: tugnait@eng.auburn.edu).

Digital Object Identifier 10.1109/TCOMM.2014.2324584

MC-MDSS, different from MC-MDIS, the strengthened subcarriers selected by the carrier bits can also carry ordinary bits. This leads to two advantages: 1) Higher spectral efficiency can be achieved than MC-MDIS due to the additional ordinary bits transmitted on the strengthened subcarriers; 2) The bit-vector-disorder issue is automatically resolved, resulting in simpler transceiver design.

It is shown that the higher spectral efficiency of MC-MDIS and MC-MDSS is achieved at a slight cost in BER performance. We would like to point out that the loss in BER performance, not significant though, may make them less favorable under low-SNR channels; however, the higher spectral efficiency achieved by MC-MDIS/MC-MDSS, as well as the ICI suppression effect of MC-MDIS, will make one or both of them popular under reasonable-SNR channels and/or in the presence of ICI.

The contributions of this paper are summarized as follows:

- First we propose a multicarrier transmission scheme with message-driven idle subcarriers (MC-MDIS). It can achieve higher spectral and power efficiency than OFDM, and also proves to be effective for ICI suppression due to the existence of idle subcarriers;
- We propose an alternative scheme with message-driven strengthened subcarriers (MC-MDSS). It can achieve an even higher spectral efficiency than MC-MDIS with slight BER performance loss;
- We provide both theoretical and numerical analysis on spectral efficiency and error probability of MC-MDIS and MC-MDSS. The simulation results match well with the theoretical calculation.

The rest of the paper is organized as follows. In Section II, the system structure of MC-MDIS is provided. In Section III, we introduce MC-MDSS. Analytical performance evaluation is presented in Section IV. Simulation results are provided in Section V and we conclude in Section VI.

II. Multicarrier Transmission With Message-Driven Idle Subcarriers (MC-MDIS)

The main idea of MC-MDIS, which distinguishes itself from MDFH [11], [15]–[18], is that part of the information bits are used to select the idle subcarriers instead of active subcarriers. The active subcarriers carry ordinary bits as usual, while for the idle ones, we transmit the carrier bits without power consumption. The essential difference between MC-MDIS and MDFH lies in: 1) MDFH only transmits information through a few selected subcarriers while keeping most subcarriers idle, leading to a lower spectral efficiency; 2) MC-MDIS is actually a "flipped" version of MDFH, which activates most of the subcarriers to transmit regular information with even the remaining idle ones carrying extra information through idle subcarrier selection, and therefore achieving a high spectral efficiency. We implement MC-MDIS through the OFDM framework to maximize the spectral efficiency.

A. Transmitter Design

Let N_c be the total number of available subcarriers, with $\{f_0, f_1, \ldots, f_{N_c-1}\}$ being the set of all available subcarrier frequencies. Here, we assume N_c is exactly a power of 2 for the convenience of OFDM implementation. All the N_c subcarriers are uniformly divided into N_g groups.[1] Within each group, there is only one idle subcarrier and the rest will carry regular symbols as usual. The number of subcarriers in each group would be $N_f = N_c/N_g$, and the number of bits required to specify the idle subcarrier in each group is $B_c = \log_2 N_f = \log_2(N_c/N_g)$. We name the bits used to specify idle subcarriers as *carrier bits*, and then the total number of carrier bits in all groups would be $N_g B_c = N_g \log_2(N_c/N_g)$.

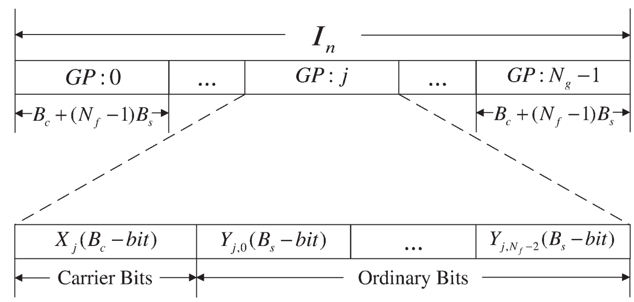

Fig. 1. Information block structure for MC-MDIS.

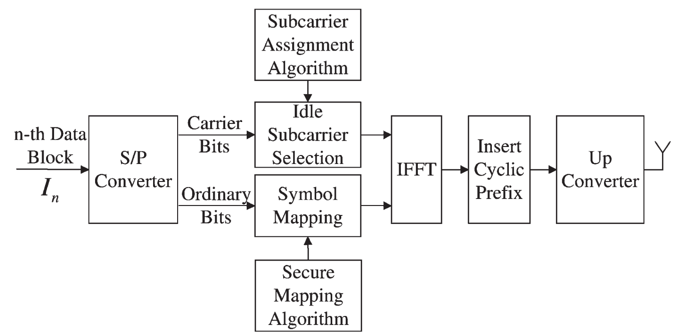

Fig. 2. Transmitter structure of MC-MDIS.

Let Ω be the selected constellation that contains M symbols, and each symbol in the constellation represents $B_s = \log_2 M$ bits. We name the bits carried in regular symbols as *ordinary bits*, and the total number of ordinary bits carried on all the active subcarriers is $(N_c - N_g)B_s = (N_c - N_g)\log_2 M$.

We divide the data stream into blocks of length $L = N_g B_c + (N_c - N_g)B_s$. Each block is partitioned into N_g groups and each group contains $B_c + (N_f - 1)B_s$ bits. The information block structure is shown in Fig. 1. We will transmit the entire block I_n, which contains L bits, in one single OFDM symbol period.

The transmitter structure is shown in Fig. 2. According to the information block structure, the Serial-to-Parallel (SP) converter fetches carrier bits and ordinary bits from the information block. The carrier bits are used to determine the idle subcarrier in each subcarrier group. The index of the idle subcarrier in the jth group, k_j, can be calculated by converting the carrier bit vector, X_j, into a decimal value, where X_j is the carrier bit vector corresponding to the idle subcarrier in the jth group. The ordinary bits are mapped to symbols which are carried by the active subcarriers.

[1] It is shown in Section IV-A and Appendix A how to properly choose N_g and why the uniform grouping strategy is optimal in terms of spectral efficiency maximization.

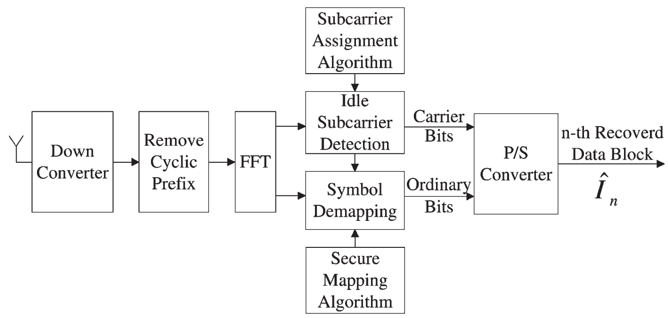

Fig. 3. Receiver structure of MC-MDIS.

Once the idle subcarriers and regular symbols are determined, we transmit the carrier bits and ordinary bits using the OFDM framework [2]. For each subcarrier, assign a zero symbol if it is idle; otherwise assign a regular symbol obtained through the bit-to-symbol mapping. If the subcarrier grouping is a direct segmentation of $\{0, 1, \ldots, N_c - 1\}$, the subcarrier index of the kth subcarrier in the jth group would be $G_{j,k} = jN_f + k$. For $i = 0, 1, \ldots, N_c - 1$, the symbol corresponding to subcarrier i is

$$d_i = d_{G_{j,k}} = \begin{cases} \mathcal{M}(Y_{j,k}), & k < k_j, \\ \mathcal{M}(Y_{j,k-1}), & k > k_j, \\ 0, & k = k_j, \end{cases} \tag{1}$$

where $\mathcal{M}(Y_{j,k})$ and $\mathcal{M}(Y_{j,k-1})$ are symbols mapped from the ordinary bit vectors $Y_{j,k}$ and $Y_{j,k-1}$, respectively. In the jth group, since the idle subcarrier indexed by k_j cannot carry an ordinary bit vector, for any $k > k_j$, subcarrier k should carry the ordinary bit vector indexed by $k - 1$ (one-vector forward). Let $d_{n,i}$ denote the ith symbol corresponding to the nth information block I_n, the OFDM symbol corresponding to I_n can then be written as [2]

$$s_n(t) = \sum_{i=0}^{N_c-1} d_{n,i} e^{j2\pi f_i t}, \quad t \in [nT_s, (n+1)T_s), \tag{2}$$

where $f_i = i/T_s$ and T_s is the OFDM symbol period. Note that the discrete version of (2) can be efficiently computed by the IFFT block in Fig. 2.

B. Receiver Design

The receiver structure is shown in Fig. 3. The nth received OFDM symbol can be written as

$$r_n(t) = s_n(t) * h(t) + n(t), \tag{3}$$

where $*$ stands for convolution, $h(t)$ is the channel impulse response, and $n(t)$ denotes additive white Gaussian noise (AWGN). Sample the OFDM symbol and remove the cyclic prefix, we get

$$r_{n,l} = r_n(t_l), \quad t_l = nT_s + l\frac{T_s}{N_c}; \quad l = 0, 1, \ldots, N_c - 1. \tag{4}$$

Performing FFT, we have

$$R_{n,i} = \sum_{l=0}^{N_c-1} r_{n,l} e^{-j2\pi f_i t_l}, \quad i = 0, 1, \ldots, N_c - 1. \tag{5}$$

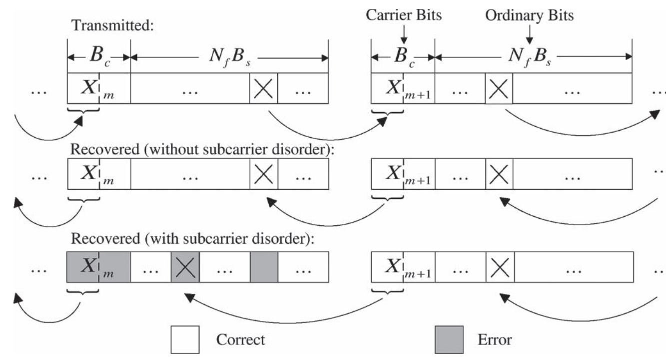

Fig. 4. Illustration of the bit vector rearrangement (BVR) algorithm.

Let $\mathbf{H} = [H(0), \ldots, H(N_c - 1)]$ be the frequency domain channel response vector. After channel estimation, the nth symbol for the ith subcarrier can be estimated as [20]

$$\hat{d}_{n,i} = \frac{R_{n,i}}{H(i)}. \tag{6}$$

Without loss of generality, the subindex n in $\hat{d}_{n,i}$ is omitted in the following discussions.

Next we look at the recovery of the carrier bits and the ordinary bits. For each subcarrier group, the idle subcarrier can be detected as

$$\hat{k}_j = \arg\min_{0 \le k \le N_f - 1} \left| \hat{d}_{G_{j,k}} \right|^2, \tag{7}$$

where $\hat{k}_j$ is the estimated index of the idle subcarrier in the jth group and $G_{j,k}$ is the shared subcarrier grouping information between the transmitter and receiver. Now the carrier bit vector, $\hat{X}_j$, can be obtained by converting the estimated idle subcarrier index, $\hat{k}_j$, into a binary carrier bit vector. After the idle subcarriers are determined, ordinary bit vectors can be estimated as

$$\begin{cases} \hat{Y}_{j,k} = \mathcal{M}^{-1}(\hat{d}_{G_{j,k}}), & k < \hat{k}_j, \\ \hat{Y}_{j,k-1} = \mathcal{M}^{-1}(\hat{d}_{G_{j,k}}), & k > \hat{k}_j, \end{cases} \tag{8}$$

where $\mathcal{M}^{-1}(\cdot)$ represents the demapping operator, $\hat{Y}_{j,k}$ and $\hat{Y}_{j,k-1}$ denote the recovered ordinary bit vectors. Hence, the entire block $\hat{I}_n$ is recovered.

C. Bit Vector Rearrangement (BVR)

One possible issue with MC-MDIS is that under low SNRs, an error in idle subcarrier detection may occur and lead to bit vector disorder in the whole subcarrier group, even if each symbol is recovered correctly from its corresponding subcarrier. To solve this problem, we develop a bit vector rearrangement (BVR) algorithm, which is described as follows and graphically illustrated in Fig. 4. Note that each information block contains N_g groups, and BVR is performed group by group rather than block by block.

Rearrangement in the transmitter:

1) Fetch $B_c + N_f B_s$ bits and determine the idle subcarrier in the current group using the first B_c bits;
2) Evacuate the B_s bits at the location of the idle subcarrier and place them at the beginning of next group;

3) Transmit the remaining $(N_f - 1)B_s$ ordinary bits on the active subcarriers of the current group;
4) Repeat the above procedures till the end of the bit stream.

Restoration in the receiver:

1) Recover both the carrier bits and ordinary bits from the current group;
2) Reserve a B_s-bit space at the location of the idle subcarrier according to the carrier bit vector in the current group;
3) Recover the next bit group and fill its first B_s bits into the reserved space in the current one;
4) Make the new group the current one and repeat from 2).

BVR is designed to keep the order of most ordinary bits from being influenced by an error in idle subcarrier detection. Note that the evacuated B_s bits in the current group will be placed at the beginning of the next one and form a carrier bit vector together with the successive $B_c - B_s$ bits. At the receiver side, each group removes its first B_s bits and fills them into the previous group, simultaneously acquiring B_s bits from the next group. As a result, the length of each group remains unchanged as $B_c + (N_f - 1)B_s$ bits. Unlike channel coding, no redundancy is introduced here, so no spectral efficiency is sacrificed. However, as in most coding methods, a mild delay will be introduced at the receiver side, since the reconstruction for the current group cannot be completed until the carrier bit vector of the next group arrives.

As shown in Fig. 4, with BVR, if an error in idle subcarrier detection occurs, only one[2] of the ordinary bit vectors in the group will be influenced, but the remaining would not. This contributes a lot to save the ordinary bits under possible idle subcarrier detection errors, especially when the group size is large. Please refer to the error probability analysis on the ordinary bits in Section IV-B for a quantitative evaluation on how much ordinary bits can be saved by BVR. In the worst case, if the carrier bits of the current group is corrupted, the first B_s bits of the next group will be placed at a wrong location. As a result, it will also lead to errors, even if they themselves are correctly recovered. However, when the group size is relatively large, the impact is insignificant comparing with the saved ordinary bits. In the case of a small group size $N_f = 2$, this approach is not recommended since no ordinary bits can be saved.

Remark 1: BVR is designed to enable MC-MDIS to work in the worst case (i.e., at low SNRs), but we would like to point out that idle subcarrier detection errors are very unlikely to occur at reasonable or high SNRs.

III. Multicarrier Transmission With Message-Driven Strengthened Subcarriers (MC-MDSS)

In this section, we introduce an alternative scheme, MC-MDSS, by replacing the idle subcarriers in MC-MDIS with strengthened ones, which transmits both carrier bits and ordinary bits. Comparing with MC-MDIS, MC-MDSS can achieve higher spectral efficiency without suffering from the bit-vector-disorder issue.

A. Transmitter Design

We use the same notations as in Section II. The first change resulted from MC-MDSS would be the information block structure. The total number of carrier bits to determine strengthened subcarriers in all groups remains unchanged as $N_g B_c = N_g \log_2(N_c/N_g)$, but the total number of ordinary bits will be increased to $N_c B_s = N_c \log_2 M$. Accordingly, in Fig. 1, the number of bits corresponding to each subcarrier group would be $B_c + N_f B_s$, and the length of the information block for MC-MDSS will be increased to $L = N_g B_c + N_c B_s$.

The power enhancement of several subcarriers make it difficult to employ non-constant-modulus[3] constellations (e.g., QAM), because under a modest amplitude-strengthening ratio, it is hard for the receiver to distinguish unamplified high-power-level symbols and amplified low-power-level symbols. For this reason, in MC-MDSS, we assume constant-modulus modulations, which can potentially be applied in digital video broadcasting [21] and optical communications [22].

Second, the idle subcarrier generation block in Fig. 2 is now replaced by the strengthened subcarrier generation block. The index of the strengthened subcarrier in the jth group, k_j, can be similarly calculated as that of idle subcarriers in MC-MDIS. A regular symbol will be assigned to each subcarrier; whereas for each strengthened subcarrier indexed by k_j, the corresponding symbol will be amplified by a fixed amplitude-strengthening ratio, γ $(\gamma > 1)$. Namely, for $i = 0, 1, \ldots, N_c - 1$, the symbol corresponding to subcarrier i is

$$d_i = d_{G_{j,k}} = \begin{cases} \gamma \mathcal{M}(Y_{j,k}), & k = k_j, \\ \mathcal{M}(Y_{j,k}), & \text{otherwise}, \end{cases} \tag{9}$$

where $\mathcal{M}(Y_{j,k})$ is the symbol mapped from the ordinary bit vector $Y_{j,k}$, and $G_{j,k}$ has the same definition as in Section II. Except the differences above, the other parts of the transmitter for MC-MDSS are exactly the same as in MC-MDIS.

B. Receiver Design

At the receiver side, we also need to make two changes for MC-MDSS accordingly. First, the block of idle subcarrier detection in Fig. 3 will be replaced by strengthened subcarrier detection. Namely, the index of the strengthened subcarrier can be determined by

$$\hat{k}_j = \underset{0 \le k \le N_f - 1}{\arg\max} \left| \hat{d}_{G_{j,k}} \right|^2. \tag{10}$$

Second, without the bit-vector-disorder issue, the ordinary bit estimation can be simplified as

$$\hat{Y}_{j,k} = \mathcal{M}^{-1}\left(\hat{d}_{G_{j,k}}\right), \tag{11}$$

where $\mathcal{M}^{-1}(\cdot)$ represents the demapping operator, and $\hat{Y}_{j,k}$ is the kth recovered ordinary bit vector in the jth subcarrier group.

[2]Note that in Fig. 4, only the middle shaded box is counted as ordinary bit errors, while the other two shaded ones are counted as carrier bit errors.

[3]For constant-modulus constellations, $\|s\|^2 = P_s$ holds for each symbol $s \in \Omega$, e.g., PSK modulation; whereas the non-constant-modulus ones do not satisfy this requirement, e.g., QAM modulation.

IV. Analytical Performance Evaluation

In this section, we analyze the performance of the two proposed schemes, MC-MDIS and MC-MDSS, in terms of spectral efficiency, power efficiency and error probability.

A. Spectral and Power Efficiency

The spectral efficiency η is defined as the ratio of the information bit rate R_b (bits/s) to the transmission bandwidth W (Hz), i.e., $\eta = R_b/W$ (bits/s/Hz). Since the proposed schemes are implemented on the OFDM framework, both of them, as well as OFDM, have the same total bandwidth $W = (N_c + 1)R_s$, where R_s is the OFDM symbol rate. To evaluate the power efficiency, we define the power ratio ρ as the ratio of the power consumed by MC-MDIS/MC-MDSS to that of OFDM.

For comparison, we first derive the bit rate $(R_{b,OFDM})$ and spectral efficiency (η_{OFDM}) of OFDM,

$$R_{b,OFDM} = R_s N_c \log_2 M, \tag{12}$$

$$\eta_{OFDM} = \frac{N_c}{N_c+1} \log_2 M \approx \log_2 M. \tag{13}$$

1) MC-MDIS: Considering both the carrier bits and the ordinary bits, the bit rate of MC-MDIS can be calculated as

$$R_{b,MDIS} = R_s \left[N_g \log_2 \frac{N_c}{N_g} + (N_c - N_g) \log_2 M \right]. \tag{14}$$

To maximize the bit rate, we differentiate (14) over N_g,

$$\frac{dR_{b,MDIS}}{dN_g} = R_s \log_2 \frac{N_c}{N_g M e}, \tag{15}$$

where e is the Euler's number. Set (15) to zero, we get $N_g^* = N_c/Me$. Note that N_g can only be a power of 2, so we select two valid candidates nearest to N_g^*: $N_{g,1}^* = N_c/2M$ and $N_{g,2}^* = N_c/4M$. Substituting them into (14), we obtain exactly the same value, which forms the maximum bit rate for MC-MDIS,

$$R_{b,MDIS}^* = R_s N_c \left[\log_2 M + \frac{1}{2M} \right]. \tag{16}$$

Although both $N_{g,1}^*$ and $N_{g,2}^*$ maximize the bit rate, we choose $N_g = N_{g,1}^* = N_c/2M$ (i.e., more subcarrier groups) due to the following two reasons: 1) For a fixed number of available subcarriers, N_c, if we choose the number of groups to be $N_c/2M$ instead of $N_c/4M$, in each group there will be only $2M$ subcarriers instead of $4M$ ones; since the idle subcarrier detection can be considered as a flipped FSK, the $2M$-ary flipped FSK would outperform the $4M$-ary one in BER performance. 2) More subcarrier groups implies more subcarriers will be left idle, which would result in further power savings and ICI suppression. With the maximized bit rate, it then follows that the maximum spectral efficiency of MC-MDIS is given by

$$\eta_{MDIS}^* = \frac{N_c}{N_c+1} \left[\log_2 M + \frac{1}{2M} \right] \approx \log_2 M + \frac{1}{2M}. \tag{17}$$

TABLE I
Comparison of Spectral and Power Efficiency

	Maximum Bit Rate	Maximum Efficiency	Efficiency Gap	Power Ratio
OFDM	$R_s N_c \log_2 M$	$\log_2 M$	N/A	N/A
MC-MDIS	$R_s N_c[\log_2 M + \frac{1}{2M}]$	$\log_2 M + \frac{1}{2M}$	$\frac{1}{2M}$	$1 - \frac{1}{2M}$
MC-MDSS	$R_s N_c[\log_2 M + \frac{1}{2}]$	$\log_2 M + \frac{1}{2}$	$\frac{1}{2}$	$\frac{\gamma^2+3}{4}$

With $N_c/2M$ out of N_c subcarriers left idle in each group, the power ratio for MC-MDIS would be

$$\rho_{MDIS} = \frac{N_c - \frac{N_c}{2M}}{N_c} = 1 - \frac{1}{2M}. \tag{18}$$

2) MC-MDSS: Similarly, the bit rate of MC-MDSS can be calculated as

$$R_{b,MDSS} = R_s \left[N_g \log_2 \frac{N_c}{N_g} + N_c \log_2 M \right]. \tag{19}$$

Using the same methodology as in MC-MDIS, by setting $N_g = N_c/4$, we obtain the maximum bit rate for MC-MDSS,

$$R_{b,MDSS}^* = R_s N_c \left[\log_2 M + \frac{1}{2} \right], \tag{20}$$

and the maximum spectral efficiency of MC-MDSS,

$$\eta_{MDSS}^* = \frac{N_c}{N_c+1} \left[\log_2 M + \frac{1}{2} \right] \approx \log_2 M + \frac{1}{2}. \tag{21}$$

With $N_c/4$ out of N_c subcarriers whose symbols will be amplified by γ in amplitude, the power ratio for MC-MDSS can be obtained as

$$\rho_{MDSS} = \frac{N_c - \frac{N_c}{4} + \gamma^2 \frac{N_c}{4}}{N_c} = \frac{\gamma^2+3}{4}. \tag{22}$$

For clarity, we summarize the analysis above in Table I. It can be seen that comparing with OFDM, the improvement achieved by MC-MDIS in both spectral efficiency and power efficiency only depends on the constellation size M, while MC-MDSS can achieve a fixed but even larger improvement in spectral efficiency than MC-MDIS at a slight cost on power efficiency.

B. Probability of Error for MC-MDIS

1) Carrier Bits: Given the average bit-level SNR, E_b/N_0, for MC-MDIS, the average symbol-level SNR, E_s/N_0, for each active subcarrier can be obtained as

$$\frac{E_s}{N_0} = \frac{L}{N_c - N_g} \frac{E_b}{N_0}, \tag{23}$$

where $L = N_g B_c + (N_c - N_g) B_s$ is the information block length and $N_c - N_g$ is the number of active subcarriers. It should be noted that E_s defined here corresponds to the average symbol energy in each active subcarrier.

The carrier bit modulation in MC-MDIS can be roughly considered as a "flipped" N_f-ary FSK, by which we mean an idle subcarrier is used to represent the carrier bits instead of an active one as in conventional FSK. Another difference is that, in MC-MDIS, when a non-constant-modulus constellation is employed, the active subcarriers may carry symbols with different power levels.

Let $E_1, \ldots, E_T$ be all the possible power levels in constellation Ω, and p_i the probability that the power level of an arbitrary symbol is E_i, then the average symbol power is given by

$$\bar{E}_s = \sum_{i=1}^{T} p_i E_i, \quad \text{where} \sum_{i=1}^{T} p_i = 1. \tag{24}$$

In this case, to achieve an overall SNR of E_s/N_0, the actual symbol-level SNR in MC-MDIS, $E_{s,i}/N_0$, would be

$$\frac{E_{s,i}}{N_0} = \frac{E_i}{\bar{E}_s}\frac{E_s}{N_0} = \frac{L}{N_c - N_g}\frac{E_i}{\bar{E}_s}\frac{E_b}{N_0}. \tag{25}$$

We can calculate the symbol error probability corresponding to the carrier bits for MC-MDIS as (see Appendix B for the details)

$$P_s^{(c)}\left(\frac{E_b}{N_0}\right) = 1 - \int_0^\infty \bar{Q}_1^{N_f-1} x e^{-\frac{x^2}{2}} dx, \tag{26}$$

in which

$$\bar{Q}_1 = \sum_{i=1}^{T} p_i Q_1\left(\sqrt{2\frac{E_{s,i}}{N_0}}, x\right), \tag{27}$$

where $Q_1(a,b) = \int_b^\infty x \exp(-(x^2+a^2)/2) I_0(ax) dx$ is the Marcum Q-function [23], in which $I_0(\cdot)$ is the zero-order modified Bessel function.

Let $P_{e,\mathrm{I}}^{(c)}$ and $P_{e,\mathrm{II}}^{(c)}$ denote the bit error probabilities for carrier bits without and with BVR, respectively. According to [24, eqn. (5.2-24), page 260],

$$P_{e,\mathrm{I}}^{(c)}\left(\frac{E_b}{N_0}\right) = \frac{2^{B_c-1}}{2^{B_c}-1} P_s^{(c)}\left(\frac{E_b}{N_0}\right). \tag{28}$$

If BVR is employed, an error in idle subcarrier detection in the current bit block will lead to an incorrect replacement of the first B_s bits within the B_c carrier bits in the successive block. If an error occurs in idle subcarrier detection for the current bit block, there are two possible results for the idle subcarrier detection in the successive block: (i) an error occurs with a probability of $P_s^{(c)}(E_b/N_0)$; or (ii) it is correctly detected with a probability of $1 - P_s^{(c)}(E_b/N_0)$. In the first case, the bit error probability would still roughly be $P_{e,\mathrm{I}}^{(c)}(E_b/N_0)$, since the B_s bits that are incorrectly replaced originally contains errors; whereas in the second case, the bit error probability will approximately become $(1 + (B_s/B_c))P_{e,\mathrm{I}}^{(c)}(E_b/N_0)$, considering the newly introduced errors resulting from the incorrectly replaced B_s bits. Combining these two cases, the bit error probability of carrier bits with BVR can be estimated as

$$P_{e,\mathrm{II}}^{(c)}\left(\frac{E_b}{N_0}\right) \approx P_s^{(c)}\left(\frac{E_b}{N_0}\right) P_{e,\mathrm{I}}^{(c)}\left(\frac{E_b}{N_0}\right) + \left(1 - P_s^{(c)}\left(\frac{E_b}{N_0}\right)\right)\left(1 + \frac{B_s}{B_c}\right) P_{e,\mathrm{I}}^{(c)}\left(\frac{E_b}{N_0}\right). \tag{29}$$

2) Ordinary Bits: The bit error probability of the ordinary bits depends on the modulation scheme exploited by the active subcarriers. We consider the case of transmitting the ordinary bits through M-ary QAM. Recall that $M = 2^{B_s}$, and the symbol error probability for M-ary QAM can be represented as[4] [24, eqn. (5.2-78) and (5.2-79), page 278]

$$P_{s,QAM}\left(\frac{E_b}{N_0}\right) = 1 - \left[1 - 2\left(1 - \frac{1}{\sqrt{M}}\right) Q\left(\sqrt{\frac{3}{M-1}\frac{E_s}{N_0}}\right)\right]^2, \tag{30}$$

where $Q(x) = (1/\sqrt{2\pi})\int_x^\infty e^{-(t^2/2)} dt$, and E_s/N_0 can be found in (23). The bit error probability of the ordinary bits on each active subcarrier can then be approximated as

$$P_{e,QAM}\left(\frac{E_b}{N_0}\right) \approx \frac{1}{B_s} P_{s,QAM}\left(\frac{E_b}{N_0}\right). \tag{31}$$

Without BVR, if an error occurs in idle subcarrier detection, there will be a bit vector disorder on all the subcarriers between the truly idle one and the incorrectly detected one, which leads to a random guess in terms of error probability. Namely, if the idle subcarrier indices selected at the transmitter and estimated at the receiver are i and j, respectively, the bit error probabilities of the ordinary bits carried on subcarrier from i through j ($|i-j|$ out of $N_f - 1$ subcarriers) would be 1/2, while the bit error probabilities of those carried on the other subcarriers will not be influenced and can thus be estimated by (31). The bit error probability of the ordinary bits with an error in idle subcarrier detection (with a probability of $P_s^{(c)}(E_b/N_0)$, in (26)) can therefore be calculated as

$$P_{e,\mathrm{I}}\left(\frac{E_b}{N_0}\right) = \sum_{i,j=0, i\neq j}^{N_f-1} \frac{1}{(N_f)_2}\left[\frac{|i-j|}{2(N_f-1)} + \left(1 - \frac{|i-j|}{N_f-1}\right) P_{e,QAM}\left(\frac{E_b}{N_0}\right)\right], \tag{32}$$

where $(n)_k$ denotes the number of k-permutations out of n.

With BVR, only one subcarrier carrying ordinary bits in each subcarrier group will be influenced and the remaining would remain uninfluenced, so the corresponding bit error probability with an error in idle subcarrier detection in this case would be

$$P_{e,\mathrm{II}}\left(\frac{E_b}{N_0}\right) = \frac{1}{2(N_f-1)} + \left(1 - \frac{1}{N_f-1}\right) P_{e,QAM}\left(\frac{E_b}{N_0}\right). \tag{33}$$

If the idle subcarrier is correctly detected, the bit error probability of the ordinary bits can also be estimated by (31). Taking all the cases into account, the bit error probability of the ordinary bits can be calculated as

$$P_{e,\kappa}^{(o)}\left(\frac{E_b}{N_0}\right) = P_s^{(c)}\left(\frac{E_b}{N_0}\right) P_{e,\kappa}\left(\frac{E_b}{N_0}\right) + \left(1 - P_s^{(c)}\left(\frac{E_b}{N_0}\right)\right) P_{e,QAM}\left(\frac{E_b}{N_0}\right), \tag{34}$$

where $\kappa \in \{\mathrm{I}, \mathrm{II}\}$ denotes whether BVR is employed or not.

[4]Note that (30) applies only when B_s is even and a rectangular constellation is employed. For cases with odd B_s or non-rectangular constellations, please refer to [24, page 278–279].

3) Overall: Following the discussions above, the overall bit error probability for MC-MDIS can be calculated as

$$P_e\left(\frac{E_b}{N_0}\right) = \frac{N_g B_c}{L} P_{e,\kappa}^{(c)}\left(\frac{E_b}{N_0}\right) + \frac{(N_c - N_g)B_s}{L} P_{e,\kappa}^{(o)}\left(\frac{E_b}{N_0}\right), \quad (35)$$

where $L = N_g B_c + (N_c - N_g)B_s$ is the number of bits in each information block for MC-MDIS, and $\kappa \in \{\mathrm{I}, \mathrm{II}\}$ denotes whether BVR is employed or not.

Remark 2: Although we analyze the error probability of MC-MDIS theoretically with QAM modulation, the constant-modulus modulation (M-ary PSK) can also be used in MC-MDIS. Using the constant-modulus modulation instead of QAM would lead to two differences: 1) The power of each active subcarrier would become identical to each other, which works as a special case of nonuniform power distribution and actually makes the calculation much easier; 2) M-ary PSK has a different representation on the error probability from that of QAM; however, concerning the error probability analysis, the only thing we need to do is to replace $P_{s,QAM}(E_b/N_0)$ with $P_{s,PSK}(E_b/N_0)$, which can be found in [24, eqn. (5.2-56), page 268].

C. Probability of Error for MC-MDSS

1) Carrier Bits: We consider the case with constant modulus constellations only. Given the average bit-level SNR, E_b/N_0, for the MC-MDSS scheme, the average symbol-level SNR, E_s/N_0, would be

$$\frac{E_s}{N_0} = L\frac{E_b}{N_0} = (N_g B_c + N_c B_s)\frac{E_b}{N_0}, \quad (36)$$

where $L = N_g B_c + N_c B_s$ is the information block length. Note that different from the definition in MC-MDIS where E_s is averaged to each active subcarrier, E_s defined here takes into account the symbols transmitted through all the subcarriers, which contains N_g strengthened subcarriers and $N_c - N_g$ regular ones. Let $E_{s,1}^{(o)}/N_0$ be the symbol-level SNR of the strengthened subcarriers, and $E_{s,2}^{(o)}/N_0$ the symbol-level SNR corresponding to those regular ones, then we have

$$N_g\frac{E_{s,1}^{(o)}}{N_0} + (N_c - N_g)\frac{E_{s,2}^{(o)}}{N_0} = \frac{E_s}{N_0}. \quad (37)$$

The power relation of the strengthened subcarriers and the regular ones can be represented as

$$\frac{E_{s,1}^{(o)}}{N_0} = \gamma^2\frac{E_{s,2}^{(o)}}{N_0}, \quad (38)$$

where γ is the amplitude-strengthening ratio which is defined in Section III. Combining (36)–(38), the SNRs for the two different kinds of subcarriers can be obtained as

$$\begin{cases} \frac{E_{s,1}^{(o)}}{N_0} = \frac{\gamma^2 L}{N_c + (\gamma^2 - 1)N_g}\frac{E_b}{N_0}, \\ \frac{E_{s,2}^{(o)}}{N_0} = \frac{L}{N_c + (\gamma^2 - 1)N_g}\frac{E_b}{N_0}. \end{cases} \quad (39)$$

The carrier bit demodulation in MC-MDSS can largely be viewed as a non-coherent N_f-ary FSK demodulation as well. What makes it slightly different from conventional FSK is that we have one strengthened subcarrier and several other regular ones (with non-zero power but less than the strengthened one), while in conventional FSK only one subcarrier has non-zero power. We can calculate the symbol error probability corresponding to the carrier bits for MC-MDSS as (see Appendix C for the details)

$$P_s^{(c)}\left(\frac{E_b}{N_0}\right) = \sum_{k=1}^{N_f - 1}(-1)^{k+1}\binom{N_f - 1}{k}\int_0^\infty \left[Q_1\left(\sqrt{2\frac{E_{s,2}^{(o)}}{N_0}}, x\right)\right]^k f\left(x \Big| \sqrt{2\frac{E_{s,1}^{(o)}}{N_0}}, 1\right)dx, \quad (40)$$

where $Q_1(a,b) = \int_b^\infty x\exp(-(x^2 + a^2)/2)I_0(ax)dx$ is the Marcum Q-function, and $f(x|\nu,\sigma) = (x/\sigma^2)\exp(-(x^2 + \nu^2)/2\sigma^2)I_0(\nu x/\sigma^2)$ denotes the probability density function of a Rician distribution. Accordingly, the bit error probability of the carrier bits can be calculated as

$$P_e^{(c)}\left(\frac{E_b}{N_0}\right) = \frac{2^{B_c - 1}}{2^{B_c} - 1}P_s^{(c)}\left(\frac{E_b}{N_0}\right). \quad (41)$$

2) Ordinary Bits: The symbol error probability of the constant-modulus modulation (PSK), $P_{s,PSK}(E_b/N_0)$, can be found in [24, eqn. (5.2-56), page 268]. What makes it different in MC-MDSS is that among all the subcarriers, N_g of them are carrying ordinary bits at the SNR of $E_{s,1}^{(o)}/N_0$, while the other $N_c - N_g$ ones work at $E_{s,2}^{(o)}/N_0$. Consequently, the symbol error probability corresponding to the ordinary bits would be

$$P_s^{(o)}\left(\frac{E_b}{N_0}\right) = \frac{N_g}{N_c}P_{s,PSK}\left(\frac{1}{B_s}\frac{E_{s,1}^{(o)}}{N_0}\right) + \frac{N_c - N_g}{N_c}P_{s,PSK}\left(\frac{1}{B_s}\frac{E_{s,2}^{(o)}}{N_0}\right). \quad (42)$$

Similarly, the bit error probability of the ordinary bits can be approximated as

$$P_e^{(o)}\left(\frac{E_b}{N_0}\right) \approx \frac{1}{B_s}P_s^{(o)}\left(\frac{E_b}{N_0}\right). \quad (43)$$

3) Overall: Following the discussions above, the overall bit error probability for MC-MDSS can be calculated as

$$P_e\left(\frac{E_b}{N_0}\right) = \frac{N_g B_c}{L}P_e^{(c)}\left(\frac{E_b}{N_0}\right) + \frac{N_c B_s}{L}P_e^{(o)}\left(\frac{E_b}{N_0}\right), \quad (44)$$

where $L = N_g B_c + N_c B_s$ is the number of bits in each information block for MC-MDSS.

V. Numerical Results

In this section, the performance of both MC-MDIS and MC-MDSS is evaluated and compared with that of OFDM and some

TABLE II
COMPARISON OF SPECTRAL EFFICIENCY WITH DIFFERENT M

Constellation Size	M	M=2	M=4	M=8	M=16
OFDM(bits/s/Hz)	$\log_2 M$	1	2	3	4
MC-MDIS(bits/s/Hz) (Compared to OFDM)	$\log_2 M + \frac{1}{2M}$	1.25 (+25%)	2.125 (+6.25%)	3.0625 (+2.08%)	4.03125 (+0.78%)
MC-MDSS(bits/s/Hz) (Compared to OFDM)	$\log_2 M + \frac{1}{2}$	1.5 (+50%)	2.5 (+25%)	3.5 (+16.7%)	4.5 (+12.5%)
CFFH(bits/s/Hz) (Compared to OFDM)	$\frac{1}{2}\log_2 M$	0.5 (-50%)	1 (-50%)	1.5 (-50%)	2 (-50%)
MDFH(bits/s/Hz) (Compared to OFDM)	$\frac{1}{2}\log_2 M + \frac{1}{2}$	1 (0%)	1.5 (-25%)	2 (-33.3%)	2.5 (-37.5%)
AJ-MDFH(bits/s/Hz) (Compared to OFDM)	$\frac{1}{2}$	0.5 (-50%)	0.5 (-75%)	0.5 (-83.3%)	0.5 (-87.5%)

other most related schemes through simulation examples. We consider both AWGN and frequency selective channels, as well as the presence of intercarrier interference (ICI). In the following, we assume $N_c = 64$, $R_s = 100$ and N_g is properly chosen according to the optimal subcarrier grouping strategy derived in Section IV-A. Unless otherwise stated, 16-QAM is used in MC-MDIS to exploit the general case of non-constant-modulus constellations, while QPSK is employed in MC-MDSS where the amplitude-strengthening ratio (γ) is set to 2. In addition, we provide the evaluation of the peak-to-average power ratio (PAPR) in Appendix D.

A. Spectral Efficiency

In Table II, for different constellation size M, we compare the spectral efficiency of the proposed MC-MDIS and MC-MDSS with that of OFDM, as well as the other most related systems in literature, including collision-free frequency hopping (CFFH) [25], message-driven frequency hopping (MDFH) [11] and anti-jamming message-driven frequency hopping (AJ-MDFH) [17]. Both MC-MDIS and MC-MDSS, with maximized efficiency, are always more efficient than the other schemes. It is also observed that the efficiency gap between MC-MDIS and OFDM decreases as the constellation size increases. It should be pointed out that the increase in bit rate achieved by MC-MDIS and MC-MDSS can be significant and of great commercial value when the baud rate is large, which is generally the case in broadband communications.

B. Bit Error Rate

1) Experimental Validation of Theoretical Results: Figs. 5 and 6 compare the theoretical and simulation BERs of both carrier bits and ordinary bits for MC-MDIS without and with BVR, respectively. Fig. 7 depicts the BERs for MC-MDSS accordingly. It can be seen that the simulation results match well with the theoretical derivation.

2) Improvement on BER by BVR for MC-MDIS: The improvement on BER by BVR for MC-MDIS is demonstrated in Fig. 8. We can see that the BER of MC-MDIS is considerably reduced by BVR, which is designed to eliminate the bit vector disorder.

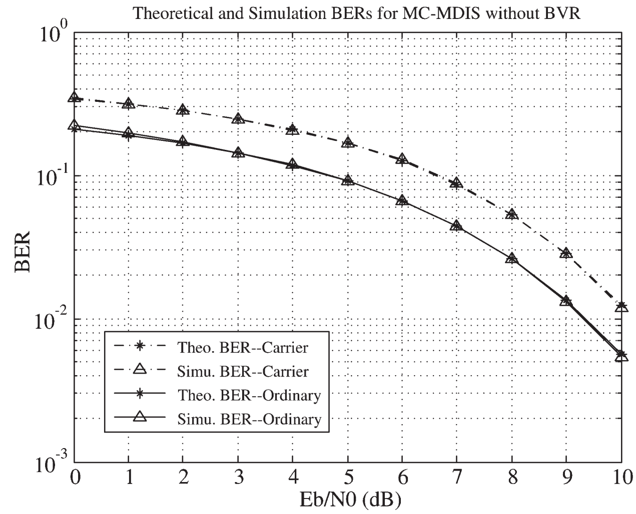

Fig. 5. Theoretical and simulation BERs for MC-MDIS without BVR.

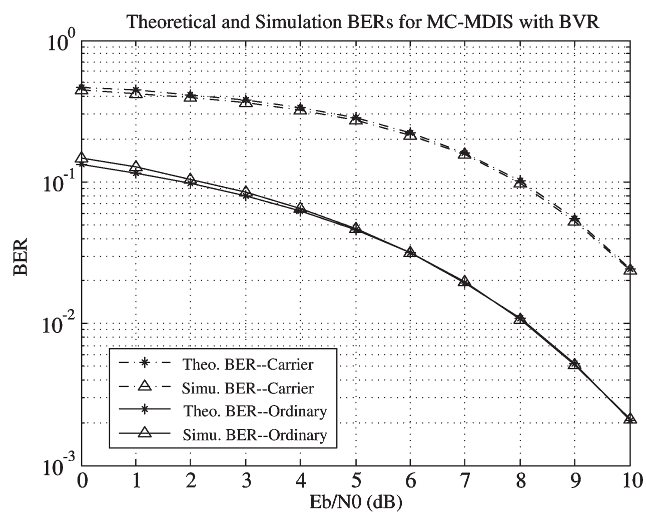

Fig. 6. Theoretical and simulation BERs for MC-MDIS with BVR.

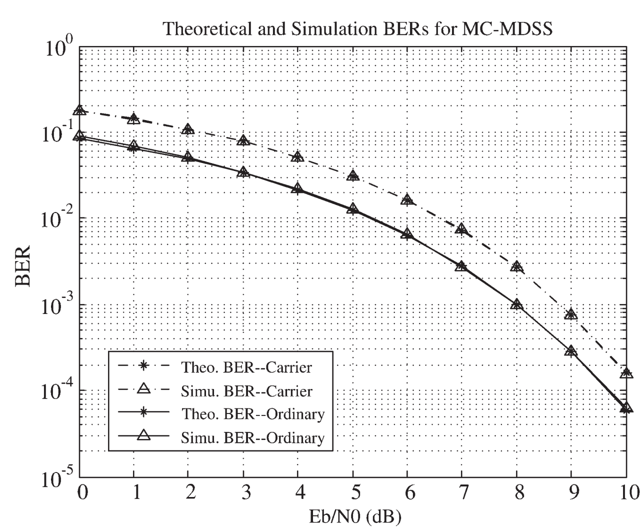

Fig. 7. Theoretical and simulation BERs for MC-MDSS.

3) BER Comparison of Different Schemes: A comprehensive BER comparison is performed involving all the schemes listed in Table II. For fair comparison, all the schemes employ

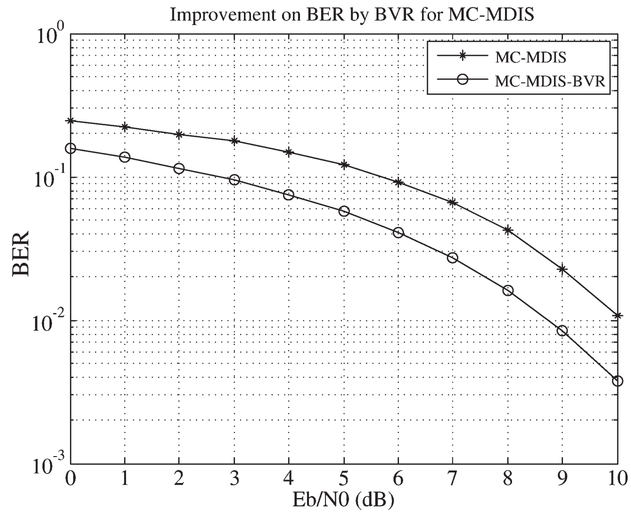

Fig. 8. Improvement on BER by BVR for MC-MDIS.

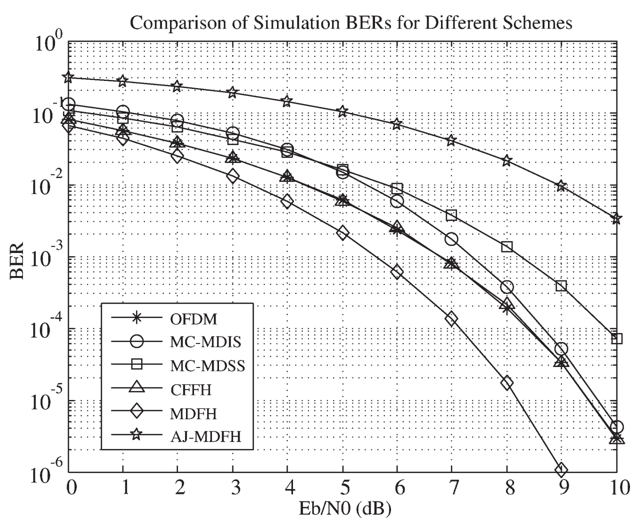

Fig. 9. Comparison of simulation BERs under AWGN channels.

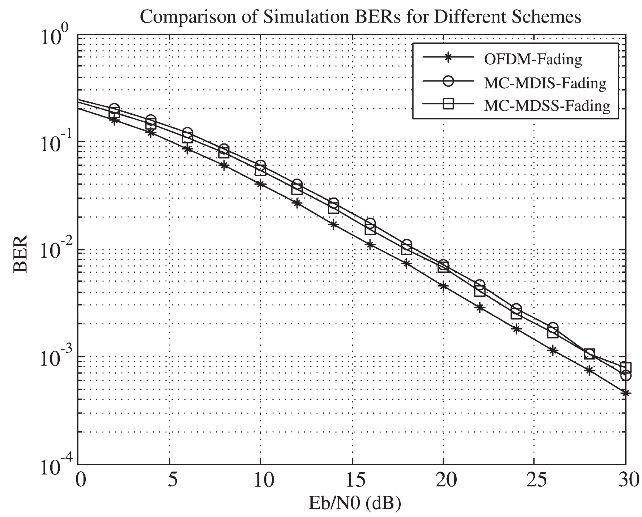

Fig. 10. Comparison of simulation BERs under frequency selective channels.

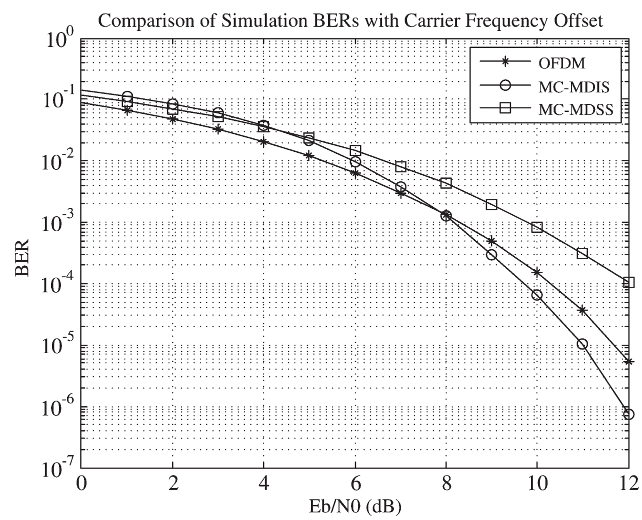

Fig. 11. Comparison of simulation BERs in the presence of ICI.

QPSK and work at their maximum bit rates, i.e., $128R_s$ for OFDM, $136R_s$ for MC-MDIS, $160R_s$ for MC-MDSS, $64R_s$ for CFFH, $96R_s$ for MDFH and $32R_s$ for AJ-MDFH, where R_s is the OFDM symbol rate.

The BER comparison under AWGN channels is shown in Fig. 9. As expected, the proposed MC-MDIS and MC-MDSS achieve higher spectral efficiency at a slight cost on BER performance, which is mainly caused by the carrier bits. It can also be observed that: 1) MC-MDSS delivers better BER performance at lower SNRs, while MC-MDIS performs better at higher SNRs (very close to OFDM), where bit vector disorder is unlikely to happen; 2) MDFH and CFFH outperform MC-MDIS and MC-MDSS in BER performance, but at the cost of considerable spectral efficiency loss (shown in Table II); 3) AJ-MDFH has an even worse BER performance, which is sacrificed together with spectral efficiency to gain the anti-jamming ability [17].

The BER comparison under a typical frequency selective channel is shown in Fig. 10. It can be observed that under frequency selective channels, neither MC-MDIS nor MC-MDSS has a larger gap to OFDM than that under AWGN channels. There is still roughly 1.0 dB gap between MC-MDIS and OFDM as under AWGN channels, and the BER performance of MC-MDSS comes even closer to OFDM than the AWGN case.

The BER comparison in the presence of intercarrier interference (ICI) is shown in Fig. 11. The residual carrier frequency offset after proper frequency synchronization/tracking [26], [27] is set to be 5 Hz, which acts as a source of ICI. It can be observed that *in the presence of ICI, MC-MDIS outperforms OFDM in terms of BER, due to the ICI suppression effect contributed by the existence of idle subcarriers*. It is expected as well as demonstrated in Fig. 11 that MC-MDSS cannot yield a better result with ICI, since it uses strengthened subcarriers instead of idle ones.

We would like to point out that the loss in BER performance of the proposed schemes (MC-MDIS/MC-MDSS), not significant though, may make them less favorable under low-SNR channels; however, the higher spectral efficiency achieved by MC-MDIS/MC-MDSS, as well as the ICI suppression effect of MC-MDIS, will make one or both of them popular under reasonable-SNR channels and/or in the presence of ICI.

VI. Conclusion

In this paper, we proposed two highly efficient OFDM-based multicarrier transmission schemes, MC-MDIS and MC-MDSS. In MC-MDIS, we specify one idle subcarrier in each group using the carrier bits, while transmits ordinary bits regularly on all the other subcarriers. Comparing with OFDM, MC-MDIS imposes no extra cost on bandwidth but resulting in higher spectral and power efficiency, as well as better ICI suppression. In MC-MDSS, the idle subcarriers are replaced by strengthened ones, which, unlike idle ones, can carry both carrier bits and ordinary bits. As a result, MC-MDSS achieves an even higher spectral efficiency than MC-MDIS with simpler transceiver design. The higher spectral efficiency achieved by MC-MDIS and MC-MDSS can be of great commercial value for broadband communications, where the baud rate is large. The loss in BER performance of the proposed schemes, not significant though, may make them less favorable under low-SNR channels; however, the higher spectral efficiency achieved by MC-MDIS/MC-MDSS, as well as the ICI suppression effect of MC-MDIS, will make one or both of them popular under reasonable-SNR channels and/or in the presence of ICI.

Appendix A
Optimality of Uniform Subcarrier Grouping

The proof here is conducted for the MC-MDIS case, but it works similarly for MC-MDSS. Suppose we have a nonuniform subcarrier grouping, and the total N_c available subcarriers are grouped into G groups, i.e.,

$$N_c = \sum_{g=0}^{G-1} N_{c,g}, \tag{45}$$

where $N_{c,g}$ denotes the number of subcarriers in the gth group. We assume $N_{c,g} \geq M$; otherwise, the idle subcarrier would not carry more information than an ordinary symbol. Please also note that $N_{c,g}$ should be a power of 2, since this is the most efficient way to carry information bits using idle subcarriers. For the gth subcarrier group, the achievable bit rate (including both carrier bits and ordinary bits) can be written as

$$\begin{aligned} R_{b,g} &= R_s \left[\log_2 N_{c,g} + (N_{c,g}-1)\log_2 M\right] \\ &= R_s \left[N_{c,g}\log_2 M + \log_2 \frac{N_{c,g}}{M}\right]. \end{aligned} \tag{46}$$

where R_s is the OFDM symbol rate. Under the assumption that $N_{c,g} \geq M$, $N_{c,g}/M = 2^n$ with $n \geq 1$. This leads to the following inequality,

$$\log_2 \frac{N_{c,g}}{M} \leq \frac{N_{c,g}}{2M}. \tag{47}$$

Substituting (47) into (46), we have

$$R_{b,g} \leq R_s N_{c,g} \left[\log_2 M + \frac{1}{2M}\right]. \tag{48}$$

Taking all the subcarrier groups into account, the total bit rate would be

$$R_b = \sum_{g=0}^{G-1} R_{b,g} \leq R_s N_c \left[\log_2 M + \frac{1}{2M}\right]. \tag{49}$$

The RHS of (49) is exactly the bit rate in (16) that the uniform subcarrier grouping can achieve, which is derived in Section IV-A. This result demonstrates that *any nonuniform subcarrier grouping would not outperform the uniform one in terms of spectral efficiency*.

Appendix B
Symbol Error Probability of Carrier Bits in MC-MDIS

In conventional FSK, the amplitude of an active subcarrier with a symbol-level SNR of E_s/N_0 obeys a Rician distribution [24, eqn. (5.4-39), page 309], and those of the other idle subcarriers follow Rayleigh distributions [24, eqn. (5.4-40), page 309]. Similarly, in MC-MDIS, we can model the amplitudes of the idle subcarrier (indexed by k_j) and the active subcarriers (with an SNR of E_s/N_0) through the following distributions,

$$f_{R_{k_j}}(r_{k_j}) = r_{k_j} \exp\left(-\frac{r_{k_j}^2}{2}\right), \tag{50}$$

$$\begin{aligned} f_{R_k}\left(r_k \middle| \sqrt{2\frac{E_s}{N_0}}, 1\right) &= r_k \exp\left[-\frac{1}{2}\left(r_k^2 + 2\frac{E_s}{N_0}\right)\right] \\ &\quad \times I_0\left(\sqrt{2\frac{E_s}{N_0}}\, r_k\right),\ k \neq k_j, \end{aligned} \tag{51}$$

respectively, where $I_0(\cdot)$ is the zero-order modified Bessel function. The probability of a correct decision, P_c, is the probability that $R_k > R_{k_j}, \forall k \neq k_j$. Hence,

$$\begin{aligned} P_c &= P(R_1 > R_{k_j}, \ldots, R_{k_j-1} > R_{k_j}, R_{k_j+1} > R_{k_j}, \\ &\qquad \ldots, R_{N_f} > R_{k_j}) \\ &= \int_0^\infty P(R_1 > R_{k_j}, \ldots, R_{k_j-1} > R_{k_j}, R_{k_j+1} > R_{k_j}, \\ &\qquad \ldots, R_{N_f} > R_{k_j} | R_{k_j} = x) f_{R_{k_j}}(x)dx. \end{aligned} \tag{52}$$

Note that $\forall k \neq k_j$, R_k's are statistically independent and identically distributed (i.i.d.), (52) can be further written as

$$P_c = \int_0^\infty \left[P(R_k > R_{k_j} | R_{k_j} = x)\right]^{N_f - 1} f_{R_{k_j}}(x)dx, \quad k \neq k_j. \tag{53}$$

We define $\bar{Q}_1 = P(R_k > R_{k_j} | R_{k_j} = x)$, and calculate it by considering all the possible power levels. Thus,

$$\begin{aligned} \bar{Q}_1 &= P(R_k > R_{k_j} | R_{k_j} = x) \\ &= \sum_{i=1}^{T} p_i \int_x^\infty f_{R_k}\left(r \middle| \sqrt{2\frac{E_{s,i}}{N_0}}, 1\right) dr \\ &= \sum_{i=1}^{T} p_i Q_1\left(\sqrt{2\frac{E_{s,i}}{N_0}}, x\right), \end{aligned} \tag{54}$$

where $Q_1(a,b) = \int_b^\infty x \exp(-(x^2+a^2)/2) I_0(ax)dx$ is the Marcum Q-function, and the definitions of p_i and $E_{s,i}/N_0$ can be found in (24), (25). Combining (50), (53), (54), the symbol error probability, which is $P_M = 1 - P_c$, becomes

$$P_M = 1 - \int_0^\infty \bar{Q}_1^{N_f-1} x e^{-\frac{x^2}{2}} dx. \tag{55}$$

APPENDIX C
SYMBOL ERROR PROBABILITY OF CARRIER BITS IN MC-MDSS

For MC-MDSS, the amplitudes of the power-strengthened subcarrier (indexed by k_j and with an SNR of $E_{s,1}^{(o)}/N_0$) and the regular ones (with an SNR of $E_{s,2}^{(o)}/N_0$) follow Rician distributions, which can be represented as

$$\begin{cases} f_{R_{k_j}}\left(r_{k_j} | \sqrt{2\frac{E_{s,1}^{(o)}}{N_0}}, 1\right) = r_{k_j} \exp\left[-\frac{1}{2}\left(r_{k_j}^2 + 2\frac{E_{s,1}^{(o)}}{N_0}\right)\right] \\ \qquad \times I_0\left(\sqrt{2\frac{E_{s,1}^{(o)}}{N_0}} r_{k_j}\right), \\ f_{R_k}\left(r_k | \sqrt{2\frac{E_{s,2}^{(o)}}{N_0}}, 1\right) = r_k \exp\left[-\frac{1}{2}\left(r_k^2 + 2\frac{E_{s,2}^{(o)}}{N_0}\right)\right] \\ \qquad \times I_0\left(\sqrt{2\frac{E_{s,2}^{(o)}}{N_0}} r_k\right), \ k \neq k_j, \end{cases} \tag{56}$$

respectively. The probability of a correct decision, P_c, is the probability that $R_{k_j} > R_k, \forall k \neq k_j$. Hence,

$$\begin{aligned} P_c &= P(R_1 < R_{k_j}, \ldots, R_{k_j-1} < R_{k_j}, R_{k_j+1} < R_{k_j}, \\ &\qquad \ldots, R_{N_f} < R_{k_j}) \\ &= \int_0^\infty P(R_1 < R_{k_j}, \ldots, R_{k_j-1} < R_{k_j}, R_{k_j+1} < R_{k_j}, \\ &\qquad \ldots, R_{N_f} < R_{k_j} | R_{k_j} = x) f_{R_{k_j}}(x) dx. \end{aligned} \tag{57}$$

Note that $\forall k \neq k_j$, R_k's are i.i.d., (57) can be further written as

$$P_c = \int_0^\infty \left[P\left(R_k < R_{k_j} | R_{k_j} = x\right)\right]^{N_f-1} f_{R_{k_j}}(x) dx, \ k \neq k_j, \tag{58}$$

where

$$P(R_k < R_{k_j} | R_{k_j} = x) = \int_0^x f_{R_k(r)} dr = 1 - Q_1\left(\sqrt{2\frac{E_{s,2}^{(o)}}{N_0}}, x\right), \tag{59}$$

in which $Q_1(a,b) = \int_b^\infty x \exp(-(x^2+a^2)/2) I_0(ax)dx$ is the Marcum Q-function. The (N_f-1)th power of (59) can then be expressed as

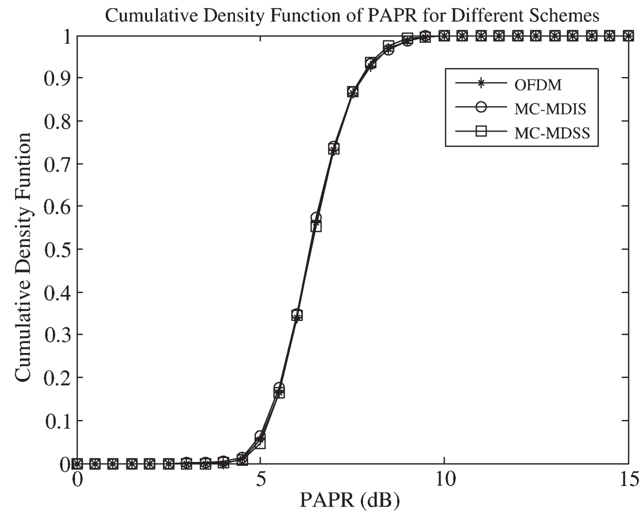

Fig. 12. Cumulative density function of PAPR for different schemes.

$$\begin{aligned} \left[1 - Q_1\left(\sqrt{2\frac{E_{s,2}^{(o)}}{N_0}}, x\right)\right]^{N_f-1} &= \sum_{k=0}^{N_f-1} (-1)^k \binom{N_f-1}{k} \\ &\quad \times \left[Q_1\left(\sqrt{2\frac{E_{s,2}^{(o)}}{N_0}}, x\right)\right]^k. \end{aligned} \tag{60}$$

Substituting (60) into (58), we obtain the probability of a correct decision as

$$\begin{aligned} P_c = \sum_{k=0}^{N_f-1} (-1)^k \binom{N_f-1}{k} \int_0^\infty \left[Q_1\left(\sqrt{2\frac{E_{s,2}^{(o)}}{N_0}}, x\right)\right]^k \\ \times f\left(x | \sqrt{2\frac{E_{s,1}^{(o)}}{N_0}}, 1\right) dx, \end{aligned} \tag{61}$$

where $f(x|\nu,\sigma) = (x/\sigma^2) \exp(-(x^2+\nu^2)/2\sigma^2) I_0(\nu x/\sigma^2)$ denotes the probability density function of a Rician distribution, which is specified in (56). Then, the symbol error probability, which is $P_M = 1 - P_c$, becomes

$$\begin{aligned} P_M = \sum_{k=1}^{N_f-1} (-1)^{k+1} \binom{N_f-1}{k} \int_0^\infty \left[Q_1\left(\sqrt{2\frac{E_{s,2}^{(o)}}{N_0}}, x\right)\right]^k \\ \times f\left(x | \sqrt{2\frac{E_{s,1}^{(o)}}{N_0}}, 1\right) dx. \end{aligned} \tag{62}$$

APPENDIX D
EVALUATION ON PEAK-TO-AVERAGE POWER RATIO (PAPR)

In Fig. 12, we provide the cumulative density functions of the peak-to-average power ratios (PAPRs) for OFDM, MC-MDIS and MC-MDSS. We can hardly see any difference among the PAPR distributions of these three schemes, which demonstrates that the proposed schemes will not suffer from higher PAPRs than OFDM.

REFERENCES

[1] B. Saltzberg, "Performance of an efficient parallel data transmission system," *IEEE Trans. Commun. Technol.*, vol. COM-15, no. 6, pp. 805–811, Dec. 1967.

[2] S. Weinstein and P. Ebert, "Data transmission by frequency-division multiplexing using the discrete Fourier transform," *IEEE Trans. Commun. Technol.*, vol. COM-19, no. 5, pp. 628–634, Oct. 1971.

[3] T. Hwang, C. Yang, G. Wu, S. Li, and G. Li, "OFDM and its wireless applications: A survey," *IEEE Trans. Veh. Technol.*, vol. 58, no. 4, pp. 1673–1694, May 2009.

[4] "Technical specification group radio access network; Evolved Universal Terrestrial Radio Access (E-UTRA) and Evolved Universal Terrestrial Radio Access Network (E-UTRAN); Overall description; Stage 2 (Release 10)," Sophia-Antipolis, France, 3GPP TS 36.300 V10.4.0 (2011-06), 2011.

[5] *IEEE Standard for Local and Metropolitan Area Networks-Part 16: Air Interface for Fixed Broadband Wireless Access Systems*, IEEE Std 802.16-2004, 2004.

[6] W. Zou and Y. Wu, "COFDM: An overview," *IEEE Trans. Broadcast.*, vol. 41, no. 1, pp. 1–8, Mar. 1995.

[7] L. Dai, J. Wang, Z. Wang, P. Tsiaflakis, and M. Moonen, "Spectrum- and energy-efficient OFDM based on simultaneous multi-channel reconstruction," *IEEE Trans. Signal Process.*, vol. 61, no. 23, pp. 6047–6059, Dec. 2013.

[8] J. Kim and Y. H. Lee, "Modified frequency-domain equalization for channel shortening in reduced-CP OFDMA systems," *IEEE Trans. Commun.*, vol. 55, no. 8, pp. 1645–1645, Aug. 2007.

[9] S. Deng *et al.*, "Reduced-guard-interval OFDM using digital sub-band-demultiplexing," *IEEE Photon. Technol. Lett.*, vol. 25, no. 22, pp. 2174–2177, Nov. 2013.

[10] A. Gusmao, P. Torres, R. Dinis, and N. Esteves, "A reduced-CP approach to SC/FDE block transmission for broadband wireless communications," *IEEE Trans. Commun.*, vol. 55, no. 4, pp. 801–809, Apr. 2007.

[11] Q. Ling and T. Li, "Message-driven frequency hopping: Design and analysis," *IEEE Trans. Wireless Commun.*, vol. 8, no. 4, pp. 1773–1782, Apr. 2009.

[12] B. Ahmadi, H. Asnani, O. Simeone, and H. Permuter, "Information embedding on actions," in *Proc. IEEE ISIT*, 2013, pp. 186–190.

[13] B. Larrousse and S. Lasaulce, "Coded power control: Performance analysis," in *Proc. IEEE ISIT*, 2013, pp. 3040–3044.

[14] R. Mesleh, H. Haas, C. W. Ahn, and S. Yun, "Spatial modulation—A new low complexity spectral efficiency enhancing technique," in *Proc. 1st Int. Conf. CHINACOM Netw.*, Oct. 2006, pp. 1–5.

[15] D. Wang, H. Zhao, and Z. Fan, "A new scheme for message-driven FH system," in *Proc. Int. Conf. Future Inf. Technol., Manage. Eng.*, Oct. 2010, vol. 2, pp. 395–398.

[16] H. Wang, L. Zhang, T. Li, and J. Tugnait, "Spectrally efficient jamming mitigation based on code-controlled frequency hopping," *IEEE Trans. Wireless Commun.*, vol. 10, no. 3, pp. 728–732, Mar. 2011.

[17] L. Zhang, H. Wang, and T. Li, "Anti-jamming message-driven frequency hopping-Part I: System design," *IEEE Trans. Wireless Commun.*, vol. 12, no. 1, pp. 70–79, Jan. 2013.

[18] L. Zhang and T. Li, "Anti-jamming message-driven frequency hopping-Part II: Capacity analysis under disguised jamming," *IEEE Trans. Wireless Commun.*, vol. 12, no. 1, pp. 80–88, Jan. 2013.

[19] G. Cooper and R. Nettleton, "A spread-spectrum technique for high-capacity mobile communications," *IEEE Trans. Veh. Technol.*, vol. VT-27, no. 4, pp. 264–275, Nov. 1978.

[20] L. Hao, T. Li, and Q. Ling, "A highly efficient secure communication interface: Collision-Free Frequency Hopping (CFFH)," in *Proc. IEEE Workshop Signal Process. Appl. Public Security Forensics*, 2007, pp. 1–4.

[21] L. Dai, Z. Wang, and Z. Yang, "Next-generation digital television terrestrial broadcasting systems: Key technologies and research trends," *IEEE Commun. Mag.*, vol. 50, no. 6, pp. 150–158, Jun. 2012.

[22] M. Selvi and K. Murugesan, "Performance of OFDM based FSO communication systems using M-ary PSK modulation," *Int. J. Comput. Appl.*, vol. 49, no. 7, pp. 41–45, Jul. 2012.

[23] P. Cantrell and A. Ojha, "Comparison of generalized Q-function algorithms," *IEEE Trans. Inf. Theory*, vol. 33, no. 4, pp. 591–596, Jul. 1987.

[24] J. G. Proakis, *Digital Communications*, 4th ed. New York, NY, USA: McGraw-Hill, 2000.

[25] L. Lightfoot, L. Zhang, J. Ren, and T. Li, "Secure collision-free frequency hopping for OFDMA-based wireless networks," *EURASIP J. Adv. Signal Process.*, vol. 2009, no. 1, p. 361063, Aug. 2009.

[26] M. Luise and R. Reggiannini, "Carrier frequency acquisition and tracking for OFDM systems," *IEEE Trans. Commun.*, vol. 44, no. 11, pp. 1590–1598, Nov. 1996.

[27] M. Morelli, C.-C. Kuo, and M.-O. Pun, "Synchronization techniques for Orthogonal Frequency Division Multiple Access (OFDMA): A tutorial review," *Proc. IEEE*, vol. 95, no. 7, pp. 1394–1427, Jul. 2007.

Tianlong Song received the B.S. degree in communication engineering from Beijing University of Chemical Technology, Beijing, China, in 2009 and the M.S. degree in information and communication engineering from Beihang University, Beijing, China, in 2012. He is currently working toward the Ph.D. degree in electrical and computer engineering in the Department of Electrical and Computer Engineering, College of Engineering, Michigan State University, East Lansing, MI, USA. His research interests include the areas of efficient and secure communications, antijamming techniques, and coding theory.

Tongtong Li received the Ph.D. degree in electrical engineering from Auburn University, Auburn, AL, USA, in 2000. From 2000 to 2002, she was with Bell Laboratories and had been working on the design and implementation of 3G and 4G systems. Since 2002, she has been with the Department of Electrical and Computer Engineering, College of Engineering, Michigan State University, East Lansing, MI, USA, where she is now an Associate Professor. Her research interests include the areas of wireless and wired communications, wireless security, information theory, and statistical signal processing. She is the recipient of the National Science Foundation Faculty Early Career Development (CAREER) Award in 2008 for her research on efficient and reliable wireless communications. She served as an Associate Editor for the IEEE SIGNAL PROCESSING LETTERS from 2007 to 2009 and as an Editorial Board Member for *EURASIP Journal Wireless Communications and Networking* from 2004 to 2011. She is currently serving as an Associate Editor for the IEEE TRANSACTIONS ON SIGNAL PROCESSING.

Jitendra K. Tugnait was born in Jabalpur, India, on December 3, 1950. He received the B.Sc.(Hons.) degree in electronics and electrical communication engineering from the Punjab Engineering College, Chandigarh, India, in 1971; the M.S. and E.E. degrees in electrical engineering from Syracuse University, Syracuse, NY, USA, in 1973 and 1974, respectively; and the Ph.D. degree in electrical engineering from the University of Illinois at Urbana–Champaign, Urbana, IL, USA, in 1978.

From 1978 to 1982, he was an Assistant Professor of electrical and computer engineering with the University of Iowa, Iowa City, IA, USA. From June 1982 to September 1989, he was with the Long Range Research Division of the Exxon Production Research Company, Houston, TX, USA. In September 1989, he joined the Department of Electrical and Computer Engineering, Samuel Ginn College of Engineering, Auburn University, Auburn, AL, USA, as a Professor, and he currently holds the title of James B. Davis Professor. His current research interests include statistical signal processing, wireless and wireline digital communications, multiple-sensor–multiple-target tracking, and stochastic systems analysis.

Dr. Tugnait was an Associate Editor of the IEEE TRANSACTIONS ON AUTOMATIC CONTROL, the IEEE TRANSACTIONS ON SIGNAL PROCESSING, the IEEE SIGNAL PROCESSING LETTERS, and the IEEE TRANSACTIONS ON WIRELESS COMMUNICATIONS. He is currently a Senior Area Editor of the IEEE TRANSACTIONS ON SIGNAL PROCESSING and a Senior Editor of the IEEE WIRELESS COMMUNICATIONS LETTERS.